Modeling and Nonlinear Heading Control of Sailing Yachts

Article *in* IEEE Journal of Oceanic Engineering · April 2014

DOI: 10.1109/JOE.2013.2247276

CITATIONS
30

READS
571

2 authors, including:

Jerome Jouffroy
University of Southern Denmark
73 PUBLICATIONS **694** CITATIONS

SEE PROFILE

Modeling and Nonlinear Heading Control of Sailing Yachts

Lin Xiao and Jerome Jouffroy

***Abstract*—This paper presents a study on the development and testing of a model-based heading controller for a sailing yacht. Using Fossen's compact notation for marine vehicles, we first describe a nonlinear four-degree-of-freedom (DOF) dynamic model for a sailing yacht, including roll. Our model also includes two possible steering mechanisms: a conventional rudder and a simple moving mass system. Starting from this model, we then design, for both steering mechanisms, a nonlinear heading controller using the integrator backstepping method, which exponentially stabilizes the heading/yaw dynamics. By computing the equilibrium points of the system, the course is related to the heading angle, and course control is also achieved. A few simulation results are presented to illustrate the behavior of our control designs.**

***Index Terms*—Course control, heading control, modeling, nonlinear feedback control, sailing yachts.**

I. Introduction

MANKIND has been sailing for thousands of years, and sailors benefit from a great deal of experience, in particular, when it comes to the relatively complex tasks of simultaneously steering the rudder on the desired course and adjusting the sail to get the best performance. This process can require great skills in the sense that it depends highly on the wind direction, but also on the sail performance, the coupling between roll and yaw, etc. Because of the challenges it presents, fully autonomous control of sailing vehicles with wind-powered propulsion is thus a topic of interest. In addition, it would also reduce the demands on sailors and increase safety at sea, and possibly extend the range of applications of autonomous sailing vessels in ocean engineering (see [1]).

Until now, there were only a few studies dedicated to automatic control of such kinds of wind-propelled vehicles. Among them, several works were based on fuzzy control theory [2], [3], neural networks [4], or other artificial intelligence techniques [5]. However, because of their underlying mathematical frameworks, none of these studies used the ship's dynamic equations, which would have allowed for further analysis. Other studies, such as [6] and [7], used a model with three degrees of freedom (DOFs) without considering the rolling motion in their controller designs, while it actually plays an important role in the behavior of yachts using the wind for propulsion. Therefore, as one of the contributions of the present paper, we propose to study the stabilization of the vehicle heading by considering a yacht model with four DOFs, including roll motion (the preliminary results were published in [8]).

In order to have an overall view on the yacht dynamics, first, we present the maneuvering model of a generic keelboat equipped with a main sail and a rudder. Masuyama *et al.* have proposed [9] a set of equations for the motion of sailing yachts expressed by the horizontal body axes system introduced by Hamamoto [10], which included hydrodynamic derivatives given by test results. This model was then tested by using parameters of an ancient Japanese sailing trader named "Naniwa-maru" [11], [12], and the numerical simulation of a wearing maneuver were in agreement with measurements from actual sea trials. As an extension of Masuyama *et al.*'s mathematical model for a tacking maneuver of a sailing yacht, Keuning *et al.* [13] reported a complete description of the forces and moments acting on the yacht considering the interactions in roll–sway–yaw. Based on the above investigations and following the way Fossen built dynamic models for marine vehicles (see [14, Ch. 2] and [15, Ch. 2 and 3]), we derived a set of equations of motion for a class of sailing yachts using a vectorial state–space representation. Our heading controller is based on the nonlinear control technique referred to as integrator backstepping, successfully applied to conventional ships (see [16]), which allows to prove that the heading error dynamics are exponentially stable.

In addition and similarly to some underwater vehicles that are partially controlled by shifting an internally located mass (see [17] and [18]), we also investigate the potential of replacing the rudder with an actuation system consisting of a simple laterally moving mass to control the ship's heading. Although our investigation can obviously be related to the well-known rudderless sailing technique, note that most works produced in this area (see, for example, [19] and [20]) considered the coordinated use of several sails to steer the ship without a rudder. In this paper, we developed our model and heading controller with the intention of letting the internal moving mass system act as the rudder, being capable of controlling the yacht's orientation, without the need to act on the sails.

After this introduction, Section II will be dedicated to the complete derivation of the dynamic equations of motion for a sailing yacht. In this section, we also model the dynamic behavior of the sail as it changes sides while tacking or jibing, as well as the introduction of a laterally moving weight system

Manuscript received January 04, 2012; revised December 20, 2012; accepted January 09, 2013.

Associate Editor: F. Hover.

The authors are with the Mads Clausen Institute, University of Southern Denmark (SDU), Sønderborg DK-6400, Denmark (e-mail: xiao@mci.sdu.dk; jerome@mci.sdu.dk).

Color versions of one or more of the figures in this paper are available online at http://ieeexplore.ieee.org.

Digital Object Identifier 10.1109/JOE.2013.2247276

TABLE I
DEFINITIONS OF VARIABLES

Notation	Description
A	plan area of the foil
AR	aspect ratio of the foil
$\boldsymbol{C}$, $\boldsymbol{C}_{RB}$, $\boldsymbol{C}_A$	system/rigid-body/added-mass Coriolis -centripetal matrix
C_D, C_L	drag and lift coefficients
C_{Di}	induced drag coefficient
CG	vehicle's center of gravity
$\boldsymbol{D}$	vector of damping
D, L	drag and lift forces acting on the foils
F, M	external forces and moments acting on the vehicle in the b-frame
F_{rh}	hull resistance
$\boldsymbol{g}$	vector of restoring forces
$\boldsymbol{I}$	principle moment of inertia in 4 DOFs in the b-frame
$\boldsymbol{J}$	coordinate transformation matrix
$\boldsymbol{M}$, $\boldsymbol{M}_{RB}$, $\boldsymbol{M}_A$	system/rigid-body/added-mass inertia matrix
M_r	static-righting moment
M_{xw}, M_{zw}	moments about the x_b/z_b-axis caused by the moving weight
$M_{\phi d}$, $M_{\psi d}$	heel/yaw-damping moment
m	total mass of the yacht
m_w	total weight of the moving mass
p, q, r	angular velocities in the b-frame
s	span of the foil
sat	saturation function
u, v, w	linear velocities in the b-frame
$\boldsymbol{v}$	vector of linear velocity in the b-frame
$\boldsymbol{v}_{tw}^b$	vector of true wind in the b-frame
v_a, α_a	apparent velocity/angle in the b-frame
v_{au}, v_{av}	apparent velocity decomposed in the longitudinal/lateral direction in the b-frame
v_{tw}, α_{tw}	true wind velocity/angle in the n-frame
$X/Y/K/N_{\dot{u}-\dot{r}}$	added mass coefficients in the b-frame
x, y	translation in the n-frame
x_w	mass position along the x_b-axis
x_m	x-coordinate of the mast in the b-frame
(x_s, y_s, z_s)	center of effort (CoE) in the b-frame with the subscripts s, r, k, and h indicate respectively the sail, rudder, keel, and hull
x_{sm}	distance between the mast and the sail's CoE
xyz	North-East-Down coordinate system (n-frame)
$x_by_bz_b$	body-fixed reference frame (b-frame)
y_{bmax}	half of the maximum yacht beam
y_w	mass position relative to the centerline of the yacht
α	angle of attack in the b-frame
γ	course angle in the n-frame
δ_r, δ_s	rudder/sail angle in the b-frame
$\bar{\delta}_s$	maximum sail angle
$\boldsymbol{\eta}$	vector of position and orientation in the n-frame
λ	leeway angle in the vessel parallel coordinate system
$\boldsymbol{\nu}$	velocity vector in the b-frame
ρ	flow density
$\boldsymbol{\tau}$	vector of propulsive forces
ϕ, ψ	Euler's angles in the n-frame
$\boldsymbol{\omega}$	angular velocity vector in the b-frame

that can be used for steering. In Section III, using the backstepping method, we introduce a model-based heading controller

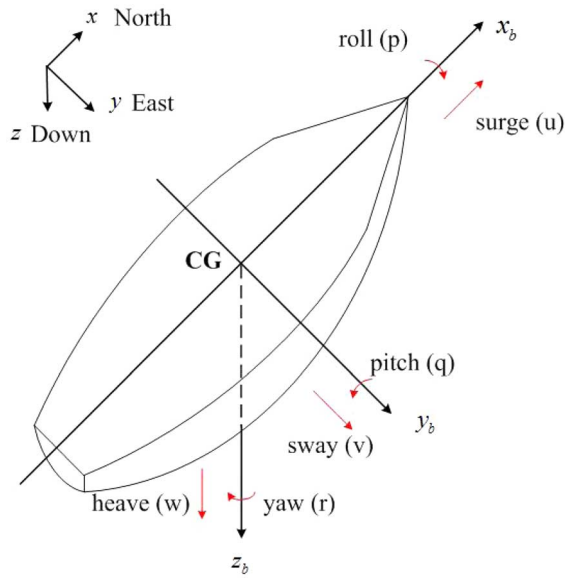

Fig. 1. Description of the coordinate systems.

that exhibits an exponential stability property with either the rudder angle or the mass position as a control input. As will be seen, it is also possible to perform course control by supplementing our heading controller with equilibrium states of the vehicle containing information on the leeway angle, as presented in Section III-D. Section III-E will introduce how to dominate the characteristic parameters of the sailing vehicle model and obtain a less parameter-dependent proportional–derivative (PD)-like controller. Afterwards, simulation results are briefly presented to illustrate the approach. Finally, a few concluding remarks end the paper.

II. DYNAMIC EQUATIONS OF MOTION

A list of the variables and parameters used in this paper is given in Table I.

A. A Four-DOF Representation in a Vectorial Form

Let the north–east–down coordinate system be the inertial reference frame (n-frame), and the body-fixed frame (b-frame) $x_by_bz_b$ is a rotating reference frame attached to the yacht (see Fig. 1), with angular velocity $\boldsymbol{\omega} = [p, q, r]^T$ relative to the n -frame. The origin of the b-frame is assumed to coincide with the yacht's center of gravity (CG).

In the following, we give a few assumptions applied throughout the paper.

1) The yacht is assumed to be rigid and four DOFs are considered, meaning we exclude both heaving and pitching motions, i.e., we have $w = q = 0$.
2) The vehicle is assumed to evolve in calm waters, i.e., the velocity of the water is zero and furthermore the motions due to waves and environmental disturbances are ignored.
3) The added mass coefficients (hydrodynamic derivatives) are computed by using the strip theory (see [14, Sec. 2.4.1]), and they are kept constant by assuming that the influence from the rolling motion is neglected.
4) The yacht is separated into parts consisting of the sail, rudder, keel, and hull, and the forces and moments acting

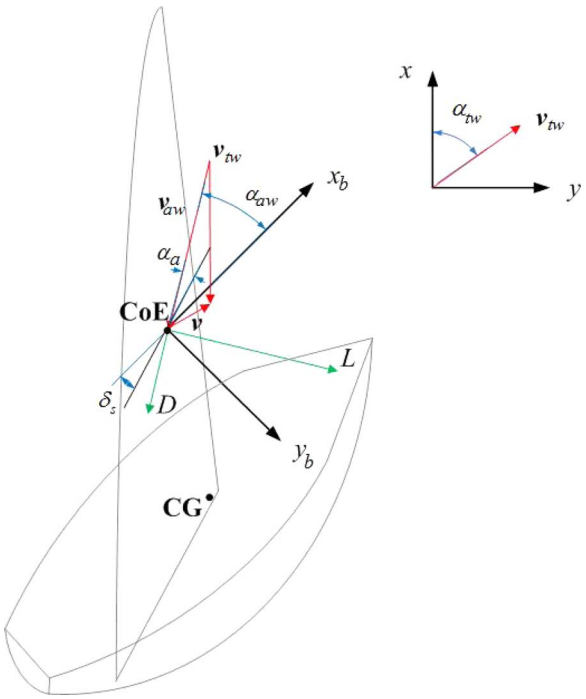

Fig. 2. Wind velocity triangle and forces on the sail.

on the yacht are the integration of the influence of each component taken separately.

5) For any foil of finite span, the flow around is 3-D and has both chordwise and spanwise velocity components (see [21, Ch. 5]). Under the thin airfoil theory and the lifting-line theory (refer to [22, Ch. 1]), the forces generated due to the interaction between the foil and the surrounding flow are acting on the quarter chord line (aerodynamic center-line or lifting line), and they vary along the span. Instead of computing the integration of the forces over the span, we assume that the resultant force is applied directly to a single point of the foil, which is referred to as the aerodynamic center of effort (see [23, p. 5], and labeled CoE in Fig. 2) and at which the total moment produced from all forces over the foil can be represented by a single force producing the same moment. In reality, the actual position of this CoE is a function of a whole series of variables, including the way in which the yacht's sail is trimmed, but we will ignore this effect and assume that the position of the CoE for each foil remains constant.

Vector $\boldsymbol{\nu} = [u, v, p, r]^T$ denotes the generalized velocity vector decomposed in the b-frame and $\boldsymbol{\eta} = [x, y, \phi, \psi]^T$ is a vector describing, respectively, the position of the yacht in the n-frame and the roll and yaw angles.

According to Newton's second law and Euler's axioms, we have $\boldsymbol{F} = m(\dot{\boldsymbol{v}} + \boldsymbol{\omega} \times \boldsymbol{v})$ and $\boldsymbol{M}_{\mathrm{CG}} = \boldsymbol{I}\dot{\boldsymbol{\omega}} + \boldsymbol{\omega} \times \boldsymbol{I}\boldsymbol{\omega}$, in which $\boldsymbol{v} = [u, v, w]^T$ and $\boldsymbol{\omega} = [p, q, r]^T$. Variables $\boldsymbol{F}$ and $\boldsymbol{M}_{\mathrm{CG}}$ are the total external forces and moments acting on the yacht, while m, the mass of the vehicle, is assumed constant. From there, we then derive the rigid-body dynamics expressed in the powerful compact vectorial setting introduced by Fossen [14], [15]

$$\boldsymbol{M}_{\mathrm{RB}}\dot{\boldsymbol{\nu}} + \boldsymbol{C}_{\mathrm{RB}}(\boldsymbol{\nu})\boldsymbol{\nu} = \boldsymbol{\tau}_{\mathrm{RB}} \tag{1}$$

where $\boldsymbol{\tau}_{\mathrm{RB}}$ is the vector of external forces and moments acting on the yacht, and where $\boldsymbol{M}_{\mathrm{RB}}$ and $\boldsymbol{C}_{\mathrm{RB}}(\boldsymbol{\nu})$ are given by

$$\boldsymbol{M}_{\mathrm{RB}} = \begin{bmatrix} m\mathbf{I}_{2\times 2} & \mathbf{0}_{2\times 2} \\ \mathbf{0}_{2\times 2} & \boldsymbol{I} \end{bmatrix}, \quad \boldsymbol{I} = \begin{bmatrix} I_{xx} & -I_{xz} \\ -I_{xz} & I_{zz} \end{bmatrix} \tag{2}$$

(where $\mathbf{I}_{2\times 2}$ is the identity matrix), and

$$\boldsymbol{C}_{\mathrm{RB}}(\boldsymbol{\nu}) = \begin{bmatrix} 0 & -mr & 0 & 0 \\ mr & 0 & 0 & 0 \\ 0 & 0 & 0 & 0 \\ 0 & 0 & 0 & 0 \end{bmatrix}. \tag{3}$$

Due to the yacht's acceleration and the inertia of the surrounding flow, there are also forces and moments coming from the so-called added mass effect. Similarly to (2) and (3), define matrices $\boldsymbol{M}_A$ and $\boldsymbol{C}_A(\boldsymbol{\nu})$ [14], [15], representing the added mass phenomenon

$$\boldsymbol{M}_A = -\begin{bmatrix} X_{\dot{u}} & X_{\dot{v}} & X_{\dot{p}} & X_{\dot{r}} \\ Y_{\dot{u}} & Y_{\dot{v}} & Y_{\dot{p}} & Y_{\dot{r}} \\ K_{\dot{u}} & K_{\dot{v}} & K_{\dot{p}} & K_{\dot{r}} \\ N_{\dot{u}} & N_{\dot{v}} & N_{\dot{p}} & N_{\dot{r}} \end{bmatrix} \tag{4}$$

$$\boldsymbol{C}_A(\boldsymbol{\nu}) = \begin{bmatrix} \mathbf{0}_{2\times 2} & \boldsymbol{C}_{A12}(\boldsymbol{\nu}) \\ \boldsymbol{C}_{A21}(\boldsymbol{\nu}) & \boldsymbol{C}_{A22}(\boldsymbol{\nu}) \end{bmatrix} \tag{5}$$

where, for example, the (negative) added mass coefficient $Y_{\dot{r}}$ represents the force in the y_b-axis due to the acceleration about the z_b-axis. Matrix $\boldsymbol{M}_A$ is strictly positive. Terms $\boldsymbol{C}_{A12}(\boldsymbol{\nu})$, $\boldsymbol{C}_{A21}(\boldsymbol{\nu})$, and $\boldsymbol{C}_{A22}(\boldsymbol{\nu})$ in (5) will be given later in this paper after simplifications of the added mass matrix [see (35)].

Defining $\boldsymbol{M} = \boldsymbol{M}_{\mathrm{RB}} + \boldsymbol{M}_A$ and $\boldsymbol{C}(\boldsymbol{\nu}) = \boldsymbol{C}_{\mathrm{RB}}(\boldsymbol{\nu}) + \boldsymbol{C}_A(\boldsymbol{\nu})$, and simultaneously considering the damping and restoring forces and moments influencing the motion of the yacht, we then have the following:

$$\boldsymbol{M}\dot{\boldsymbol{\nu}} + \boldsymbol{C}(\boldsymbol{\nu})\boldsymbol{\nu} + \boldsymbol{D}(\boldsymbol{\nu}, \boldsymbol{\eta}) + \boldsymbol{g}(\boldsymbol{\eta}) = \boldsymbol{\tau} \tag{6}$$

where $\boldsymbol{D}(\boldsymbol{\nu}, \boldsymbol{\eta})$ is the damping matrix, $\boldsymbol{g}(\boldsymbol{\eta})$ contains the restoring forces, while $\boldsymbol{\tau}$ is a vector related to the forces and moments used to control the vehicle, i.e., the forces generated from the sail and rudder. Vector $\boldsymbol{\eta}$ is then derived through a coordinate transformation [14], [15], giving

$$\dot{\boldsymbol{\eta}} = \boldsymbol{J}(\boldsymbol{\eta})\boldsymbol{\nu} \tag{7}$$

with $\boldsymbol{J}(\boldsymbol{\eta})$ defined as

$$\boldsymbol{J}(\boldsymbol{\eta}) = \begin{bmatrix} \boldsymbol{J}_1(\boldsymbol{\eta}) & \mathbf{0}_{2\times 2} \\ \mathbf{0}_{2\times 2} & \boldsymbol{J}_2(\boldsymbol{\eta}) \end{bmatrix} \tag{8}$$

$$\boldsymbol{J}_1(\boldsymbol{\eta}) = \begin{bmatrix} \cos\psi & -\sin\psi\cos\phi \\ \sin\psi & \cos\psi\cos\phi \end{bmatrix} \tag{9}$$

$$\boldsymbol{J}_2(\boldsymbol{\eta}) = \begin{bmatrix} 1 & 0 \\ 0 & \cos\phi \end{bmatrix}. \tag{10}$$

As will be seen in Section II-B, vector τ is itself a function of vectors $\boldsymbol{\eta}$ and $\boldsymbol{\nu}$, but also of the control inputs that are the rudder angle δ_r and the sail angle δ_s, as well as the wind velocity and direction v_{tw} and α_{tw}, respectively, i.e., we have $\boldsymbol{\tau}(\boldsymbol{\eta}, \boldsymbol{\nu}, \delta_r, \delta_s, v_{\mathrm{tw}}, \alpha_{\mathrm{tw}})$. Hence, putting together (6) and (7), and

using the fact that matrix $\boldsymbol{M}$ is invertible, we can easily put our yacht model into the following state–space representation:

$$\dot{\boldsymbol{\eta}} = \boldsymbol{J}(\boldsymbol{\eta})\boldsymbol{\nu} \tag{11}$$

$$\dot{\boldsymbol{\nu}} = -\boldsymbol{M}^{-1}\boldsymbol{C}(\boldsymbol{\nu})\boldsymbol{\nu} - \boldsymbol{M}^{-1}\boldsymbol{D}(\boldsymbol{\nu},\boldsymbol{\eta}) - \boldsymbol{M}^{-1}\boldsymbol{g}(\boldsymbol{\eta}) + \boldsymbol{M}^{-1}\boldsymbol{\tau}(\boldsymbol{\eta},\boldsymbol{\nu},\delta_r,\delta_s,v_{\rm tw},\alpha_{\rm tw}). \tag{12}$$

B. Forces and Moments Induced by the Moving Appendages

In this section, we now turn to the derivation of terms $\boldsymbol{g}(\boldsymbol{\eta})$, $\boldsymbol{D}(\boldsymbol{\nu},\boldsymbol{\eta})$, and $\boldsymbol{\tau}$ of representation (6).

In our case, $\boldsymbol{g}(\boldsymbol{\eta})$ comprises the static-righting moment $M_r(\phi)$, which represents the moment forcing the yacht upright at a given heel angle when it is stationary in the water. The heel-damping moment $M_{\phi d}(\dot{\phi})$ and the yaw-damping moment $M_{\psi d}(\dot{\psi})$, which oppose the rotational motions in roll and yaw, together with the forces from the keel and the hull account for the damping vector $\boldsymbol{D}$ in (6). Typically, terms $M_r(\phi)$, $M_{\phi d}(\dot{\phi})$, and $M_{\psi d}(\dot{\psi})$ can be obtained by fitting a quadratic in ϕ, $\dot{\phi}$, and $\dot{\psi}$, respectively (see, for example, [24]). As a consequence, we have

$$\boldsymbol{g}(\boldsymbol{\eta}) = \begin{bmatrix} 0 \\ 0 \\ M_r(\phi) \\ 0 \end{bmatrix} = \begin{bmatrix} 0 \\ 0 \\ a\phi^2 + b\phi \\ 0 \end{bmatrix} \tag{13}$$

with a and b the constant coefficients to be determined by performing an inclining test on the yacht. On the other hand, the quadratic damping related to the heeling and yawing motions is

$$\boldsymbol{D}_{\rm heel}(\boldsymbol{\nu}) + \boldsymbol{D}_{\rm yaw}(\boldsymbol{\nu},\boldsymbol{\eta}) = \begin{bmatrix} 0 \\ 0 \\ M_{\phi d}(\dot{\phi}) \\ M_{\psi d}(\dot{\psi})\cos\phi \end{bmatrix} = \begin{bmatrix} 0 \\ 0 \\ c\dot{\phi}|\dot{\phi}| \\ d\dot{\psi}|\dot{\psi}|\cos\phi \end{bmatrix}. \tag{14}$$

Because of the yacht's heeling, the yaw-damping moment $M_{\psi d}(\dot{\psi})$ has components about the y_b- and z_b-axes, hence the presence of term $\cos\phi$ in (14).

As mentioned in assumption 4), each part of the yacht (sail, rudder, and keel) is regarded as a thin foil such that the basic aerohydrodynamic theory can be applied. As a yacht is generally controlled by the motions of the sail and the rudder, we group in vector $\boldsymbol{\tau}$ [from (6)] the terms linked to the important variables that are the sail angle δ_s and the rudder angle δ_r, here considered as control inputs.

From aerohydrodynamics, the lift and drag forces acting on a foil are

$$L = \frac{1}{2}\,\rho\,A\,v_a^2\,C_L(\alpha) \tag{15}$$

$$D = \frac{1}{2}\,\rho\,A\,v_a^2\,C_D(\alpha) \tag{16}$$

where α is the angle of attack between the apparent incoming flow and the foil, C_L and C_D are the lift and drag coefficients as functions of α, both of which are obtained from appropriate measurements (e.g., wind tunnel for an airfoil). Constant A represents the plan area of the foil.

The interaction between the sail and the wind generates the propulsive power of the yacht. As can be seen in Fig. 2, the apparent wind $\boldsymbol{v}_{\rm aw}$ as seen by the sail is the vector sum of the so-called true wind and the yacht velocity, i.e., $\boldsymbol{v}_{\rm aw} = \boldsymbol{v}_{\rm tw}^b - \boldsymbol{v}$, where vectors $\boldsymbol{v}_{\rm aw}$ and $\boldsymbol{v}$ are defined in the b-frame while $\boldsymbol{v}_{\rm tw}$ is in the n-frame, i.e., $\boldsymbol{v}_{\rm tw}^n = [v_{\rm tw}\cos\alpha_{\rm tw}, v_{\rm tw}\sin\alpha_{\rm tw}]^T$ with $v_{\rm tw}$ the magnitude of the wind and $\alpha_{\rm tw}$ its direction.

However, in a 3-D setting, the apparent velocity vector should also incorporate the effect induced by the rotation of the yacht. Hence, we have

$$\boldsymbol{v}_{\rm aw} = \boldsymbol{v}_{\rm tw}^b - \boldsymbol{v} - \boldsymbol{\omega} \times [x_s, y_s, z_s]^T \tag{17}$$

where $[x_s, y_s, z_s]^T$ is the position of the CoE of the sail,[1] and $\boldsymbol{v}_{\rm tw}^n = [v_{\rm tw}\cos\alpha_{\rm tw}, v_{\rm tw}\sin\alpha_{\rm tw}, 0]^T$. Thus, in the b-frame, we have $\boldsymbol{v}_{\rm tw}^b = \mathbf{R_2}\mathbf{R_1}\boldsymbol{v}_{\rm tw}^n$ with $\mathbf{R_1}$ and $\mathbf{R_2}$

$$\mathbf{R_1} = \begin{bmatrix} \cos(-\psi) & -\sin(-\psi) & 0 \\ \sin(-\psi) & \cos(-\psi) & 0 \\ 0 & 0 & 1 \end{bmatrix} \tag{18}$$

$$\mathbf{R_2} = \begin{bmatrix} 1 & 0 & 0 \\ 0 & \cos(-\phi) & -\sin(-\phi) \\ 0 & \sin(-\phi) & \cos(-\phi) \end{bmatrix}. \tag{19}$$

Rewriting (17) in a component form in the x_by_b-plane, we get

$$\begin{aligned} v_{awu} &= v_{\rm tw}\cos(\alpha_{\rm tw} - \psi) - u + ry_s \\ v_{awv} &= v_{\rm tw}\sin(\alpha_{\rm tw} - \psi)\cos\phi - v - rx_s + pz_s \end{aligned} \tag{20}$$

where v_{awu} and v_{awv} are the apparent wind velocity along the longitudinal and lateral axes in the b-frame. Hence, we have $v_{\rm aw} = \sqrt{v_{awu}^2 + v_{awv}^2}$, while the apparent wind angle in the b-frame is $\alpha_{\rm aw} = \arctan 2(v_{awv}, -v_{awu})$.[2] Then, the angle of attack for the sail is given by

$$\alpha_s(\boldsymbol{\eta},\boldsymbol{\nu},\delta_s,v_{\rm tw},\alpha_{\rm tw}) = \alpha_{\rm aw}(\boldsymbol{\eta},\boldsymbol{\nu},v_{\rm tw},\alpha_{\rm tw}) - \delta_s \tag{21}$$

which, in turn, gives the value of lift and drag coefficients $C_{\rm Ls}(\alpha_s)$ and $C_{\rm Ds}(\alpha_s)$. These can finally be used to get the lift and drag forces L_s and D_s, generated by the sail, obtained from (15) and (16). However, the flow around a foil of finite span will produce trailing vortices [21], which results in an additional drag component termed induced drag (or the vortex drag), so that we have $C_D(\alpha) = C_D(\alpha) + C_{\rm Di}(\alpha)$ with (see [25, pp. 367–375])

$$C_{\rm Di}(\alpha) = \frac{C_L^2(\alpha)}{\pi AR}, \quad AR = \frac{s^2}{A}. \tag{22}$$

[1]Similarly, the CoE of the rudder, keel, and hull will be noted (x_r, y_r, z_r), (x_k, y_k, z_k), and (x_h, y_h, z_h), respectively.

[2]$\arctan 2(y, x)$ is a four-quadrant inverse tangent of the real parts of y and x, and $\arctan 2(y, x) \in [-\pi, \pi]$.

Note that (22) will also be used when calculating the drag from the rudder and keel. Hereby, the forces and moments generated by the sail (with notation with suffix s) are expressed as

$$\begin{aligned}&\boldsymbol{\tau}_s(\boldsymbol{\eta},\boldsymbol{\nu},\delta_s,v_{\rm tw},\alpha_{\rm tw})\\&=\begin{bmatrix}F_{xs}\\F_{ys}\\M_{xs}\\M_{zs}\end{bmatrix}\\&=\begin{bmatrix}L_s\sin\alpha_{\rm aw}-D_s\cos\alpha_{\rm aw}\\L_s\cos\alpha_{\rm aw}+D_s\sin\alpha_{\rm aw}\\(L_s\cos\alpha_{\rm aw}+D_s\sin\alpha_{\rm aw})|z_s|\\-(L_s\sin\alpha_{\rm aw}-D_s\cos\alpha_{\rm aw})x_{\rm sm}\sin\delta_s\\+(L_s\cos\alpha_{\rm aw}+D_s\sin\alpha_{\rm aw})(x_m-x_{\rm sm}\cos\delta_s)\end{bmatrix}\end{aligned}\tag{23}$$

where $x_{\rm sm}$ is the distance between the mast and the sail's CoE, while x_m is the x-coordinate of the mast in the b-frame.

Similarly to (20), the apparent velocity of the water (note that the true water velocity is assumed to be zero, i.e., there is no current) on the rudder is given by

$$\begin{aligned}v_{aru}&=-u+ry_r\\v_{arv}&=-v-rx_r+pz_r\end{aligned}\tag{24}$$

and $\alpha_r(\boldsymbol{\nu},\delta_r)=\alpha_{\rm ar}(\boldsymbol{\nu})-\delta_r$. Accordingly, we have

$$\boldsymbol{\tau}_r(\boldsymbol{\nu},\delta_r)=\begin{bmatrix}F_{xr}\\F_{yr}\\M_{xr}\\M_{zr}\end{bmatrix}=\begin{bmatrix}L_r\sin\alpha_{\rm ar}-D_r\cos\alpha_{\rm ar}\\L_r\cos\alpha_{\rm ar}+D_r\sin\alpha_{\rm ar}\\(L_r\cos\alpha_{\rm ar}+D_r\sin\alpha_{\rm ar})|z_r|\\-(L_r\cos\alpha_{\rm ar}+D_r\sin\alpha_{\rm ar})|x_r|\end{bmatrix}\tag{25}$$

where we assume that the CG of the yacht (i.e., the origin of the b-frame) is below the CoE of the rudder, so that the absolute value of z_r is used in (25). Consequently, combining (23) and (25), we can derive a complete expression for the vector $\boldsymbol{\tau}$, i.e., $\boldsymbol{\tau}(\boldsymbol{\eta},\boldsymbol{\nu},\delta_r,\delta_s,v_{\rm tw},\alpha_{\rm tw})=\boldsymbol{\tau}_s(\boldsymbol{\eta},\boldsymbol{\nu},\delta_s,v_{\rm tw},\alpha_{\rm tw})+\boldsymbol{\tau}_r(\boldsymbol{\nu},\delta_r)$.

Similarly again, the forces and moments arising from the keel are

$$\boldsymbol{D}_k(\boldsymbol{\nu})=\begin{bmatrix}F_{xk}\\F_{yk}\\M_{xk}\\M_{zk}\end{bmatrix}=\begin{bmatrix}-L_k\sin\alpha_{ak}+D_k\cos\alpha_{ak}\\-L_k\cos\alpha_{ak}-D_k\sin\alpha_{ak}\\(-L_k\cos\alpha_{ak}-D_k\sin\alpha_{ak})|z_k|\\(L_k\cos\alpha_{ak}+D_k\sin\alpha_{ak})|x_k|\end{bmatrix}\tag{26}$$

with the apparent velocity

$$\begin{aligned}v_{aku}&=-u+ry_k\\v_{akv}&=-v-rx_k+pz_k\end{aligned}\tag{27}$$

and $\alpha_k=\alpha_{ak}=\arctan 2(v_{akv},-v_{aku})$.

With regard to hull forces, the so-called extended keel method is used, whereby the lift force generated by the hull is accounted for by extending the keel and rudder inside the yacht body to the waterline [26]. As a result, in the so-called hull resistance force $F_{\rm rh}(v_{ah})$, only the drag component is considered, and it is increasing with the apparent velocity of the flow on the hull in the vessel parallel coordinate system, i.e., the plane parallel to the water surface

$$\begin{aligned}v_{ahx}&=-u+ry_h\\v_{ahy}&=(-v-rx_h+pz_h)\sec\phi\end{aligned}\tag{28}$$

which gives $v_{ah}=\sqrt{v_{ahx}^2+v_{ahy}^2}$ and $\alpha_{ah}=\arctan 2(v_{ahy},-v_{ahx})$, leading to

$$\boldsymbol{D}_h(\boldsymbol{\nu},\boldsymbol{\eta})=\begin{bmatrix}F_{xh}\\F_{yh}\\M_{xh}\\M_{zh}\end{bmatrix}=\begin{bmatrix}F_{\rm rh}(v_{ah})\cos\alpha_{ah}\\-F_{\rm rh}(v_{ah})\sin\alpha_{ah}\cos\phi\\(-F_{\rm rh}(v_{ah})\sin\alpha_{ah}\cos\phi)|z_h|\\F_{\rm rh}(v_{ah})\sin\alpha_{ah}\cos\phi|x_h|\end{bmatrix}.\tag{29}$$

As a consequence, the damping vector is finally given by $\boldsymbol{D}(\boldsymbol{\nu},\boldsymbol{\eta})=\boldsymbol{D}_k(\boldsymbol{\nu})+\boldsymbol{D}_h(\boldsymbol{\nu},\boldsymbol{\eta})+\boldsymbol{D}_{\rm heel}(\boldsymbol{\nu})+\boldsymbol{D}_{\rm yaw}(\boldsymbol{\nu},\boldsymbol{\eta})$.

C. Modeling of a Sail Luffing

In addition to the above few terms, another feature of our model is that it also includes the behavior of the sail as it changes sides while tacking or jibing. Indeed, while in a tacking maneuver, the sail typically loses lift and starts flapping or luffing.

Considering that the sail angle is constrained by a rope connecting the sail (or usually the boom) with the boat, denote by $\bar{\delta}_s$ the maximum sail angle that can be obtained on the yacht given a particular rope length, i.e., $|\delta_s|\leq\bar{\delta}_s$. In a tacking maneuver, the tension of the rope disappears, letting the rope loose while the heading of the boat is in the no-sailing zone. In this situation, a reasonable approximation consists in considering that the sail is aligned with the apparent wind until it catches the wind again, i.e., $\alpha_s(\boldsymbol{\eta},\boldsymbol{\nu},\delta_s,v_{\rm tw},\alpha_{\rm tw})=0$ in (21).

As a result, the possibility for the sail of being either tight or luffing in the wind can be simply represented by

$$\delta_s=\mathrm{sat}^{\bar{\delta}_s}_{-\bar{\delta}_s}(\alpha_{\rm aw})\tag{30}$$

where sat is the saturation function. Note that online tuning of $\bar{\delta}_s$ can be considered, and it is indeed what is usually done in practice by changing the rope length. In this case, a control input for the yacht model is not δ_s, but $\bar{\delta}_s$, the maximum sail angle determined by the rope length.

D. Internal Moving Mass System

As is well known for smaller sailboats such as dinghies, moving a weight inside or on the hull (such as the crew, for example) also contributes to the turning moments as it moves laterally from one side to the other, and can thus contribute to steering. Introduce a variable y_w, seen here as a control input, which ranges from -1 to 1 to represent the mass position relative to the yacht centerline, i.e., $y_w=0$, such that the mass actuation system is set in a way that the aerodynamic and hydrodynamic forces result in no turning moment.

The turning moments coming from the moving mass system can then be approximated by [24]

$$M_{xw}=y_w m_w y_{\rm bmax}\cos\phi\tag{31}$$

$$M_{zw}=y_w m_w x_w\sin|\phi|\tag{32}$$

where m_w is the weight of the movable mass in Newtons, y_{bmax} is half of the maximum yacht beam, and x_w is the position of the weight along the x_b-axis. Accordingly, (31) and (32) should be incorporated into vector $\boldsymbol{\tau}$ from (6) as

$$\boldsymbol{\tau}_w(\boldsymbol{\eta}, y_w) = \begin{bmatrix} 0 \\ 0 \\ M_{xw} \\ M_{zw} \end{bmatrix} \tag{33}$$

and in that case, in (12), vector $\boldsymbol{\tau}$ also depends on y_w, i.e., we have $\boldsymbol{\tau}(\boldsymbol{\eta}, \boldsymbol{\nu}, \delta_r, \delta_s, y_w, v_{\mathrm{tw}}, \alpha_{\mathrm{tw}})$.

III. Model-Based Heading Control

A. Model Simplifications

In the added mass matrix given in (4), not all of the terms have an evident impact on the forces and moments due to added mass effect. In this case, it is possible to simplify (4) to a form which is more convenient computationally.

Considering the yacht to be symmetrical about the $x_b z_b$-plane and the fact that $\boldsymbol{M}_{Aij} = \boldsymbol{M}_{Aji}$ gives [14], [15]

$$\boldsymbol{M}_A = -\begin{bmatrix} X_{\dot{u}} & 0 & 0 & 0 \\ 0 & Y_{\dot{v}} & Y_{\dot{p}} & Y_{\dot{r}} \\ 0 & Y_{\dot{p}} & K_{\dot{p}} & K_{\dot{r}} \\ 0 & Y_{\dot{r}} & K_{\dot{r}} & N_{\dot{r}} \end{bmatrix}. \tag{34}$$

Thus, the matrices in (5) are now

$$\begin{aligned} \boldsymbol{C}_{A12}(\boldsymbol{\nu}) &= \begin{bmatrix} 0 & Y_{\dot{v}} v + Y_{\dot{p}} p + Y_{\dot{r}} r \\ 0 & -X_{\dot{u}} u \end{bmatrix} \\ \boldsymbol{C}_{A21}(\boldsymbol{\nu}) &= \begin{bmatrix} 0 & 0 \\ -Y_{\dot{v}} v - Y_{\dot{p}} p - Y_{\dot{r}} r & X_{\dot{u}} u \end{bmatrix} \\ \boldsymbol{C}_{A22}(\boldsymbol{\nu}) &= [\mathbf{0}_{2\times 2}]. \end{aligned} \tag{35}$$

For further simplification, we also considered that the smaller off-diagonal terms of (2) and (34) could be neglected for the purpose of controller design, while they can be kept to simulate the real plant dynamics (see also [27] for an interesting discussion on the distinction and roles of process plant and control plant models). As a result, we rewrite $\boldsymbol{M}_{\mathrm{RB}} = \mathrm{diag}\{m, m, I_{xx}, I_{zz}\}$ and $\boldsymbol{M}_A = -\mathrm{diag}\{X_{\dot{u}}, Y_{\dot{v}}, K_{\dot{p}}, N_{\dot{r}}\}$, while $\boldsymbol{C}_A(\boldsymbol{\nu})$ is now written as

$$\boldsymbol{C}_A(\boldsymbol{\nu}) = \begin{bmatrix} 0 & 0 & 0 & Y_{\dot{v}} v \\ 0 & 0 & 0 & -X_{\dot{u}} u \\ 0 & 0 & 0 & 0 \\ -Y_{\dot{v}} v & X_{\dot{u}} u & 0 & 0 \end{bmatrix}.$$

In addition, a further simplification can be obtained by assuming that the apparent angle of the water on the rudder is very small, i.e., $\alpha_{\mathrm{ar}} \approx 0$, so we get $\cos\alpha_{\mathrm{ar}} \approx 1$ and $\sin\alpha_{\mathrm{ar}} \approx 0$. Therefore, the forces and moments coming from the rudder are (see also [28] where a similar simplification is used)

$$\boldsymbol{\tau}_r(\boldsymbol{\nu}, \delta_r) = \begin{bmatrix} F_{xr} \\ F_{yr} \\ M_{xr} \\ M_{zr} \end{bmatrix} = \begin{bmatrix} -D_r \\ L_r \\ L_r |z_r| \\ -L_r |x_r| \end{bmatrix}. \tag{36}$$

The above simplifications will be used throughout the remainder of this section.

B. Nonlinear Heading Controller Design

The control objective is to find a feedback law that exponentially stabilizes the heading ψ of the yacht around a chosen constant desired heading ψ_d. In this section, we investigate the heading/yaw subdynamics of system (6)–(7), and then design a heading controller using the backstepping method by using two different steering systems that are the rudder and the internal moving mass. The rudder will be first considered below (i.e., in this case, we have $y_w = 0$).

From (6)–(7), we extract the following heading/yaw subdynamics:

$$\begin{aligned} \dot{\psi} &= r\cos\phi \\ \dot{r} &= f(\psi, r, \delta_r, \delta_s, u, v, p, \phi) \end{aligned} \tag{37}$$

where $[\psi, r]^T \in [-\pi, \pi] \times \mathbb{R}$ is the state and $\delta_r \in [-\pi/3, \pi/3]$ is the control input, while δ_s, u, v, p, ϕ can be seen as disturbances to system (37). We then consider the stabilization of the nonlinear dynamical system (37) around its equilibrium points, whose stability is usually characterized in the sense of Lyapunov [29, pp. 33–79], [30, Ch. 5]. To do so, we will make use of the integrator backstepping method [31], [32, Ch. 14].

Considering again system (37), perform now a change of coordinate and define a new state $z_1 = \psi - \psi_d$ representing the error in heading with $\dot{\psi}_d = 0$, for which we obtain the new dynamics $\dot{z}_1 = r\cos\phi$.

Using the backstepping technique, we first choose r as the virtual control input to stabilize the scalar system $\dot{z}_1 = r\cos\phi$ at the origin $z_1 = 0$, with a stabilizing function $\alpha_1(z_1)$ such that $\dot{V}_1 < 0$ for all $z_1 \neq 0$, where V_1 is a Lyapunov function candidate. Using the control Lyapunov function (CLF) $V_1 = z_1^2/2$, we obtain

$$\dot{V}_1 = z_1 \alpha_1 \cos\phi. \tag{38}$$

We then set $\alpha_1(z_1) = -k_1 z_1$, where $k_1 > 0$ is the feedback gain, which gives $\dot{V}_1 = -k_1 \cos\phi z_1^2$. Here, $\phi \in]-\pi/2, \pi/2[$ leads to $\cos\phi > 0$.

However, since r is not an actual control input, we can achieve $r = \alpha_1(z_1)$ only with an error, represented by the new variable $z_2 = r - \alpha_1(z_1)$. Thus

$$\dot{z}_1 = (z_2 + \alpha_1(z_1))\cos\phi \tag{39}$$

and $\dot{V}_1$ is rewritten as

$$\dot{V}_1 = z_1(z_2 + \alpha_1(z_1))\cos\phi = -k_1\cos\phi z_1^2 + z_1 z_2 \cos\phi \tag{40}$$

while the z_2-dynamics is

$$\dot{z}_2 = f - \dot{\alpha}_1(z_1), \quad \dot{\alpha}_1(z_1) = -k_1 r\cos\phi. \tag{41}$$

Picking the CLF candidate for a system composed of (39) and (41) as $V_2 = V_1 + z_2^2/2$, together with (40), we obtain

$$\dot{V}_2 = -k_1\cos\phi z_1^2 + z_1 z_2 \cos\phi + z_2(f + k_1 r\cos\phi). \tag{42}$$

Then, letting $f = -k_1 r\cos\phi - z_1\cos\phi - k_2 z_2 = -(k_1\cos\phi + k_2)r - (\cos\phi + k_1 k_2)(\psi - \psi_d)$ with $k_2 > 0$ guarantees that $\dot{V}_2 = -k_1\cos\phi z_1^2 - k_2 z_2^2 < 0, \forall z_1 \neq 0, z_2 \neq 0$.

From the model derived in Section II and by making use of the control plant model after simplifications, we have

$$\begin{aligned} &f(\psi, r, \delta_r, \delta_s, u, v, p, \phi) \\ &\quad = ((-X_{\dot{u}} + Y_{\dot{v}})uv - M_{\psi d}(\dot{\psi})\cos\phi \\ &\qquad + M_{zs}(\psi, r, \delta_s, u, v, p, \phi) + M_{zr}(r, \delta_r, u, v, p) \\ &\qquad - M_{zk}(r, u, v, p) - M_{zh}(r, u, v, p, \phi))/(I_{zz} - N_{\dot{r}}). \end{aligned} \tag{43}$$

Equating (43) with $-(k_1\cos\phi + k_2)r - (\cos\phi + k_1k_2)(\psi - \psi_d)$ and using (14), (23), (36), (26), and (29), we obtain

$$\begin{aligned} C_{\mathrm{Lr}}(\alpha_r) = &((-(k_1\cos\phi + k_2)r - (\cos\phi + k_1k_2)(\psi - \psi_d)) \\ &\times (I_{zz} - N_{\dot{r}}) - (-X_{\dot{u}} + Y_{\dot{v}})uv + M_{\psi d}(\dot{\psi})\cos\phi \\ &- M_{zs}(\psi, r, \delta_s, u, v, p, \phi) + M_{zk}(r, u, v, p) \\ &+ M_{zh}(r, u, v, p, \phi)) \Big/ \left(-\frac{|x_r|}{2}\rho_w A_r v_{\mathrm{ar}}^2\right) \end{aligned} \tag{44}$$

where C_{Lr}, the lift coefficient for the rudder, is a function of the angle of attack α_r. Since $\alpha_r = \alpha_{\mathrm{ar}} - \delta_r$, then control input δ_r can finally be obtained as

$$\delta_r = \alpha_{\mathrm{ar}} - C_{\mathrm{Lr}}^{-1} \tag{45}$$

where C_{Lr}^{-1} is the inverse of function $C_{\mathrm{Lr}}(\alpha_r)$ as defined in (44).

Note that the range of the rudder lift coefficient function $C_{\mathrm{Lr}}(\alpha_r)$ is generally bounded, as can be seen, for example, in Fig. 12 in the Appendix. This, in turn, means that this function can only be locally invertible, thus giving a nonglobal aspect to the controller with regard to exponential stability, as summarized in the following result.

Theorem 1: Given the nonlinear model-based rudder controller derived from (44) and (45), system (37) in closed loop is uniformly locally exponentially stable (ULES) around a desired heading.

Proof: It follows from the above backstepping design procedure that the resulting dynamics of the closed-loop system in $\boldsymbol{z} = [z_1, z_2]^T$ can be written as

$$\begin{bmatrix} \dot{z}_1 \\ \dot{z}_2 \end{bmatrix} = -\begin{bmatrix} k_1\cos\phi & 0 \\ 0 & k_2 \end{bmatrix}\begin{bmatrix} z_1 \\ z_2 \end{bmatrix} + \begin{bmatrix} 0 & \cos\phi \\ -\cos\phi & 0 \end{bmatrix}\begin{bmatrix} z_1 \\ z_2 \end{bmatrix}. \tag{46}$$

Choose the Lyapunov function $V(\boldsymbol{z}) = (1/2)\boldsymbol{z}^T\boldsymbol{z}$, which after time differentiation leads to $\dot{V}(\boldsymbol{z}) = -\boldsymbol{z}^T K \boldsymbol{z}$, where $K = \mathrm{diag}\{k_1\cos\phi, k_2\} > 0$. Hence, the origin of (39) and (41), i.e., $(z_1, z_2) = (0, 0)$, is exponentially stable according to the Lyapunov theory, which in turn implies exponential stability of the original system (37) around a desired heading. Local exponential stability is verified in the range of function $C_{\mathrm{Lr}}(\alpha_r)$ in (44).

Note that in the above result, the local aspect of the exponential stability could be expected, the impact of the rudder, as well as the forces of propulsion of the yacht (namely, the wind) are limited, whereas global exponential generally corresponds to potentially very large control inputs whenever the initial conditions are far from the steady state. However, our investigations have shown that the domain of attraction of the proposed controller is more than sufficiently large for implementation.

C. Controller Design Using the Moving Mass System

Alternatively, set $\delta_r = 0$ and use only the movement of the mass from port to starboard to steer the yacht. Hence, considering the contribution of the mass weight to the yacht dynamics, the heading/yaw subdynamics in (37) is as shown in (47), at the bottom of the page, with minor changes in the yaw dynamics, where the mass-turning moment M_{zw} is given in (32) and $y_w \in [-1, 1]$ is the control input.

Theorem 2: Given the internal moving mass controller defined in (49), the system in (47) is ULES around a desired heading.

Proof: Similarly to the derivations of the previous section, we want to have

$$\begin{aligned} &f(\psi, r, y_w, \delta_s, u, v, p, \phi) \\ &\qquad = -(k_1\cos\phi + k_2)r - (\cos\phi + k_1k_2)(\psi - \psi_d) \end{aligned} \tag{48}$$

from (47) by following similar steps to Section III-B, with k_1, k_2 positive and ψ_d the desired heading. As a consequence, the controller expression is then obtained as

$$\begin{aligned} y_w = &((-(k_1\cos\phi + k_2)r - (\cos\phi + k_1k_2)(\psi - \psi_d)) \\ &\times (I_{zz} + N_{\dot{r}}) - (-X_{\dot{u}} + Y_{\dot{v}})uv + M_{\psi d}(\dot{\psi})\cos\phi \\ &- M_{zs} - M_{zr} + M_{zk} + M_{zh})/(m_w x_w \sin|\phi|). \end{aligned} \tag{49}$$

□

D. Course Control

1) Sailing and the Leeway Angle: Typically, a sailing yacht does not longer sail in the direction of its longitudinal axis but in a direction slightly to leeward because of the side force generated from the interaction between the sail and the wind. As a consequence, the yacht follows the course, albeit with an error due to the leeway angle, denoted here as λ.

The angle λ, by which the yacht speed along the course direction in the parallel plane is deviated with respect to the longitudinal axis, depends on the yacht speed and heel, and is defined as

$$\lambda = \arctan 2(v/\cos\phi, u). \tag{50}$$

Accordingly, the course angle γ is obtained in the inertial coordinate system

$$\gamma = \psi + \arctan 2(v/\cos\phi, u). \tag{51}$$

2) Equilibrium States and Course Control: Since (51) relates the heading angle ψ to the course direction γ, it is

$$\begin{aligned} \dot{\psi} &= r\cos\phi \\ \dot{r} &= f(\psi, r, y_w, \delta_s, u, v, p, \phi) \\ &= \frac{(-X_{\dot{u}} + Y_{\dot{v}})uv - M_{\psi d}(\dot{\psi})\cos\phi + M_{zs} + M_{zr} + M_{zw} - M_{zk} - M_{zh}}{I_{zz} + N_{\dot{r}}} \end{aligned} \tag{47}$$

feasible to develop course controllers, which might have more practical interest for sailing vehicles because of the presence of the leeway angle, instead of the heading controllers derived in Sections III-B and III-C. The main idea consists in computing the heading angle ψ_d corresponding to a desired course direction γ_d for a sailing yacht in steady state. Then, ψ_d is passed to our previously obtained heading controllers.

In order to find ψ_d, we need to find the equilibrium points for dynamics (6)–(7). Using Matlab function $fsolve$, we are able to find these equilibrium points (which are grouped in $[u^*, v^*, \phi^*, \psi_d, \delta_r^*]^T$ or $[u^*, v^*, \phi^*, \psi_d, y_w^*]^T$ for different means of steering) given the constraint (51) and the desired course angle γ_d, and obtain ψ_d for a specific tuning of the sail, i.e., a maximum sail angle $\overline{\delta}_s$.

E. Heading Control Using Parameters Tuning

1) Domination of the System Characteristic Coefficients: As can be seen in Sections III-B and III-C, our model-based heading controllers depend on the main characteristics of sailing yachts such as lift/drag coefficients, damping terms, etc., which are normally obtained through experimentation on physical models or/and in conjunction with numerical methods (e.g., computational fluid dynamics (CFD) [23]). However, experimentation in test tanks and wind tunnels is not always suitable due to time and cost constraints. Hence, it would be of interest to obtain controllers that, while maintaining good performances, rely less on the system model.

To do so, we use hereafter the backstepping method again, but this time take the feedback term that will dominate some characteristic terms, which is inspired by [33] by using sine functions to dominate the lift and drag coefficients.

To begin with, we detail (43) further, giving

$$\begin{aligned} &f(\psi, r, \delta_r, \delta_s, u, v, p, \phi) \\ &= \frac{1}{I_{zz} - N_{\dot r}}((-X_{\dot u} + Y_{\dot v})uv - M_{\psi d}(\dot\psi)\cos\phi + M_{zs} + M_{zr}) \\ &= \frac{1}{I_{zz} - N_{\dot r}}\Bigg((-X_{\dot u} + Y_{\dot v})uv - d\dot\psi|\dot\psi|\cos\phi + \frac{1}{2}\rho_a A_s v_{\rm aw}^2 \\ &\qquad \times ((C_{\rm Ls}(\alpha_s)\cos\alpha_{\rm aw} + C_{\rm Ds}(\alpha_s)\sin\alpha_{\rm aw}) \\ &\qquad\quad \times (x_m - x_{\rm sm}\cos\delta_s) \\ &\qquad\quad - (C_{\rm Ls}(\alpha_s)\sin\alpha_{\rm aw} - C_{\rm Ds}(\alpha_s)\cos\alpha_{\rm aw}) \\ &\qquad\quad \times x_{\rm sm}\sin\delta_s) \\ &\qquad - \frac{|x_r|}{2}\rho_w A_r v_{\rm ar}^2 C_{\rm Lr}(\alpha_r)\Bigg). \end{aligned} \tag{52}$$

Rewrite now (42) as follows:

$$\begin{aligned} \dot V_2 &= -k_1\cos\phi z_1^2 - z_2^2 \\ &\quad + z_2(f + z_1\cos\phi + z_2 + k_1 r\cos\phi) \\ &= -k_1\cos\phi z_1^2 - (1-\theta)z_2^2 \\ &\quad + z_2(f + z_1\cos\phi + z_2 + k_1 r\cos\phi) - \theta z_2^2 \end{aligned} \tag{53}$$

where constant parameter θ is such that $0 < \theta < 1$. Obviously, $z_2(f + z_1\cos\phi + z_2 + k_1 r\cos\phi) - \theta z_2^2 \le 0$ ensures $\dot V_2 \le -k_1\cos\phi z_1^2 - (1-\theta)z_2^2 \le 0$. In the following, we need to find the appropriate control input δ_r such that $z_2(f + z_1\cos\phi + z_2 + k_1 r\cos\phi) \le \theta z_2^2$ to make $\dot V_2$ negative for all $z_1 \neq 0, z_2 \neq 0$.

Because $z_2(f + z_1\cos\phi + z_2 + k_1 r\cos\phi) \le |z_2||f + z_1\cos\phi + z_2 + k_1 r\cos\phi|$, then it is sufficient to prove $|z_2||f + z_1\cos\phi + z_2 + k_1 r\cos\phi| \le \theta z_2^2$, i.e., to find $|f + z_1\cos\phi + z_2 + k_1 r\cos\phi| \le \theta|z_2|$.

Let f_1 be function $f + z_1\cos\phi + z_2 + k_1 r\cos\phi$, thus

$$|f_1| \le \left|\frac{d}{I_{zz} - N_{\dot r}}\dot\psi\left|\dot\psi\right|\cos\phi\right| + |f_1'| \tag{54}$$

where function f_1' is f_1, excluding the yaw-damping term. Due to the property of the absolute value $|R_1 - R_2| \ge ||R_1| - |R_2||$, where R_1, R_2 are two real numbers, we have the following inequality:

$$\left||f_1'| - \left|\frac{K_{\rm yaw}}{I_{zz} - N_{\dot r}}\dot\psi|\dot\psi|\cos\phi\right|\right| \le \left|f_1' - \frac{K_{\rm yaw}}{I_{zz} - N_{\dot r}}\dot\psi|\dot\psi|\cos\phi\right| \tag{55}$$

in which $K_{\rm yaw}$ is a constant ($K_{\rm yaw} \in \mathbb{R}$) to be tuned such that the following condition is satisfied:

$$\left|\frac{d}{I_{zz} - N_{\dot r}}\dot\psi|\dot\psi|\cos\phi\right| + |f_1'| \le \left||f_1'| - \left|\frac{K_{\rm yaw}}{I_{zz} - N_{\dot r}}\dot\psi|\dot\psi|\cos\phi\right|\right| \tag{56}$$

i.e.,

$$\left|\frac{K_{\rm yaw}}{I_{zz} - N_{\dot r}}\dot\psi|\dot\psi|\cos\phi\right| - \left|\frac{d}{I_{zz} - N_{\dot r}}\dot\psi|\dot\psi|\cos\phi\right| \ge 2|f_1'|. \tag{57}$$

Considering again (54)–(56), condition (57) for tuning the yaw-damping coefficient $K_{\rm yaw}$ leads to $|f_1| \le |f_1' - (K_{\rm yaw})/(I_{zz} - N_{\dot r})\dot\psi|\dot\psi|\cos\phi|$.

Take again $f_1' - (K_{\rm yaw})/(I_{zz} - N_{\dot r})\dot\psi|\dot\psi|\cos\phi$ as a function f_2 and similarly to (54)

$$|f_2| \le \left|\frac{M_{zr}}{I_{zz} - N_{\dot r}}\right| + |f_2'| \tag{58}$$

together with the other inequality

$$\begin{aligned} &\left||f_2'| - \left|\frac{K_{\rm lr}|x_r|}{2(I_{zz} - N_{\dot r})}\rho_w A_r v_{\rm ar}^2\sin\alpha_r\right|\right| \\ &\qquad \le \left|f_2' - \frac{K_{\rm lr}|x_r|}{2(I_{zz} - N_{\dot r})}\rho_w A_r v_{\rm ar}^2\sin\alpha_r\right| \end{aligned} \tag{59}$$

where $K_{\rm lr} \in \mathbb{R}^+$ is a constant parameter to be tuned. Condition $|(K_{\rm lr}|x_r|)/(2(I_{zz} - N_{\dot r}))\rho_w A_r v_{\rm ar}^2\sin\alpha_r| - |(|x_r|)/(2(I_{zz} - N_{\dot r}))\rho_w A_r v_{\rm ar}^2 C_{\rm Lr}(\alpha_r)| \ge 2|f_2'|$ guarantees that $|f_2| \le |f_2' - (K_{\rm lr}|x_r|)/(2(I_{zz} - N_{\dot r}))\rho_w A_r v_{\rm ar}^2\sin\alpha_r|$.

Analogously, choose a sine function $K_{\rm ls}\sin\alpha_s$ to represent the lift coefficient $C_{\rm Ls}(\alpha_s)$ while another function defined as $K_{d0} + K_{\rm ds}\sin^2\alpha_s$ (see [33]) is used to denote the sail drag coefficient $C_{\rm Ds}(\alpha_s)$. In the end, we get $|f_1| \le |g + z_1\cos\phi + z_2 + k_1 r\cos\phi|$, where g is the function after dominations of the coefficients.

Finally, the controller can be designed such that $|g + z_1\cos\phi + z_2 + k_1 r\cos\phi| \le \theta|z_2|$, i.e., $-\theta|z_2| \le g + z_1\cos\phi + z_2 + k_1 r\cos\phi \le \theta|z_2|$. Choose $g + z_1\cos\phi + z_2 + k_1 r\cos\phi = 0$, then δ_r is derived in (60) by equating function g to $-(z_1\cos\phi + z_2 + k_1 r\cos\phi)$, i.e.,

$$\begin{aligned} &\delta_r(\psi, r, \delta_s, u, v, p, \phi) \\ &= \alpha_{\rm ar} - \arcsin\Bigg(\Big((-(1 + k_1\cos\phi)r \; - (k_1 + \cos\phi)(\psi - \psi_d)\Big) \end{aligned}$$

$$
\begin{aligned}
&\times (I_{zz} - N_{\dot{r}}) - (-X_{\dot{u}} + Y_{\dot{v}})uv \\
&+ K_{\text{yaw}} r|r| \cos^3\phi - \frac{1}{2}\rho_a A_s v_{\text{aw}}^2 \\
&\times ((K_{\text{ls}} \sin\alpha_s \cos\alpha_{\text{aw}} \\
&\quad + (K_{d0} + K_{\text{ds}} \sin^2\alpha_s) \sin\alpha_{\text{aw}}) \\
&\quad \times (x_m - x_{\text{sm}} \cos\delta_s) \\
&\quad - (K_{\text{ls}} \sin\alpha_s \sin\alpha_{\text{aw}} \\
&\quad\quad - (K_{d0} + K_{\text{ds}} \sin^2\alpha_s) \cos\alpha_{\text{aw}}) \\
&\times x_{\text{sm}} \sin\delta_s)\Big) \Big/ \left(-K_{\text{lr}} \frac{|x_r|}{2} \rho_w A_r v_{\text{ar}}^2\right)\Big)
\end{aligned} \tag{60}
$$

with k_1 positive, ψ_d the desired heading, and the constant parameters K_{yaw}, K_{ls}, K_{d0}, K_{ds}, and K_{lr} to be tuned.

Hence, the above derivations can be summarized in the following theorem.

Theorem 3: Given the nonlinear model-based rudder controller defined in (60), the system with unknown aerohydrodynamic and yaw damping coefficients in (37) is ULES around a desired heading.

Furthermore, the above approach is also valid for heading control using the moving mass system, as the only differences lie in the expressions of functions f and g. Indeed, in this case, we have

$$
\begin{aligned}
&y_w(\psi, r, \delta_s, u, v, p, \phi) \\
&= \Big((-(1 + k_1\cos\phi)r - (k_1 + \cos\phi)(\psi - \psi_d)) \\
&\quad \times (I_{zz} - N_{\dot{r}}) - (-X_{\dot{u}} + Y_{\dot{v}})uv + K_{\text{yaw}} r|r| \cos^3\phi \\
&\quad - \frac{1}{2}\rho_a A_s v_{\text{aw}}^2 \\
&\quad \times ((K_{\text{ls}} \sin\alpha_s \cos\alpha_{\text{aw}} + (K_{d0} + K_{\text{ds}} \sin^2\alpha_s) \sin\alpha_{\text{aw}}) \\
&\quad\quad \times (x_m - x_{\text{sm}} \cos\delta_s) \\
&\quad\quad - (K_{\text{ls}} \sin\alpha_s \sin\alpha_{\text{aw}} \\
&\quad\quad\quad - (K_{d0} + K_{\text{ds}} \sin^2\alpha_s) \cos\alpha_{\text{aw}}) x_{\text{sm}} \sin\delta_s) \\
&\quad + K_{\text{lr}} \frac{|x_r|}{2} \rho_w A_r v_{\text{ar}}^2 \sin\alpha_r\Big) \Big/ (m_w x_w \sin|\phi|)
\end{aligned} \tag{61}
$$

with k_1 positive, ψ_d the desired heading, and the constant parameters K_{yaw}, K_{ls}, K_{d0}, K_{ds}, and K_{lr} to be tuned.

Theorem 4: Given the internal moving mass controller defined in (61), the system with unknown aerohydrodynamic and yaw damping coefficients in (47) is ULES around a desired heading.

2) Tuning Method: In this way, it is possible to use the control algorithm proposed in this paper even if the model is partially known (e.g., the yaw-damping coefficient and the aerohydrodynamic coefficients are unknown). By tuning the five parameters, the controller (δ_r or y_w) is capable of providing control action to minimize the error in heading.

As can be seen in control laws (60) and (61), the controllers play a role analogous to that of a nonlinear PD controller [34, Ch. 10], with K_{yaw} acting as the D-term while the others (K_{ls}, K_{d0}, K_{ds}, and K_{lr}) are more akin to P values. Similarly to the tuning methods used for PD controllers [35], a series of adjustment guidelines are presented in the following for the proposed heading controllers.

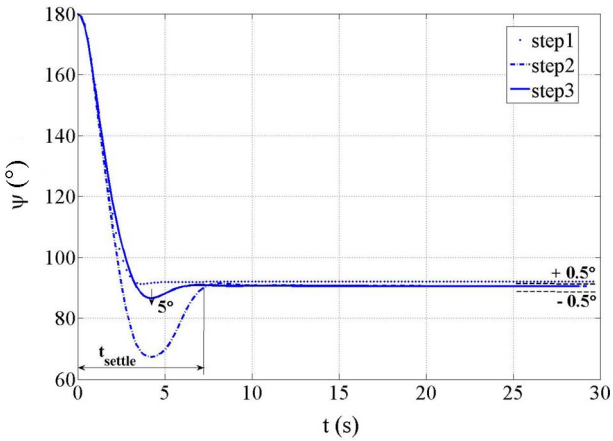

Fig. 3. Representation of parameters tuning.

Fig. 4. Graphic representation of our yacht model in a 3-D environment.

For this study, note that we used the parameters given in the Appendix. First, set K_{yaw} to zero. Second, from many references (e.g., [23], [36], and [37]), it appears that the foil is always such that its lift/drag coefficient is within some boundaries. For this study, we take $|C_L| < 2$ and $0 < C_D < 1.5$. Then, we use these values as the first step to tune the remaining parameters, e.g., set $K_{\text{ls}} = K_{\text{lr}} = 2$ and $K_{\text{ds}} = 1.5$. Besides, K_{d0} is normally small compared to the other parameters, so that K_{d0} is set to 0.1 and kept unchanged.

Afterwards, we adjust only K_{lr} to see the system response and decide whether to raise or to decrease it to reduce the error $\psi - \psi_d$. We stop tuning K_{lr} when the system oscillates too much (it depends on the specific requirement on the overshoot). Finally, we tune K_{yaw} to make the system more damped.

As an illustration, we followed the above steps to tune these parameters so as to achieve heading control, with initial values $[x, y, \phi, \psi, u, v, p, r]^T(0) = [0, 0, 0, \pi, 5, 0, 0, 0]^T$ and $\psi_d = 90°$. In addition, it is required that the steady-state error is $\pm 0.5°$ due to the simplified control model, the overshoot is less than 5°, and the settling time is less than 10 s.

As shown by the dotted line in Fig. 3, the system has an error of more than 0.5° when the controller is tuned with $K_{\text{yaw}} = 0, K_{\text{ls}} = K_{\text{lr}} = 2, K_{\text{ds}} = 1.5$ and $K_{d0} = 0.1$. However, the overshoot is quite small and the system is extraordinary stable in this case. The dashed–dotted line represents an obvious big oscillation at the beginning due to the increase on K_{lr} during the second tuning step ($K_{\text{lr}} = 4.5$), but the steady-state error is now below the required performance value. Finally, we tune

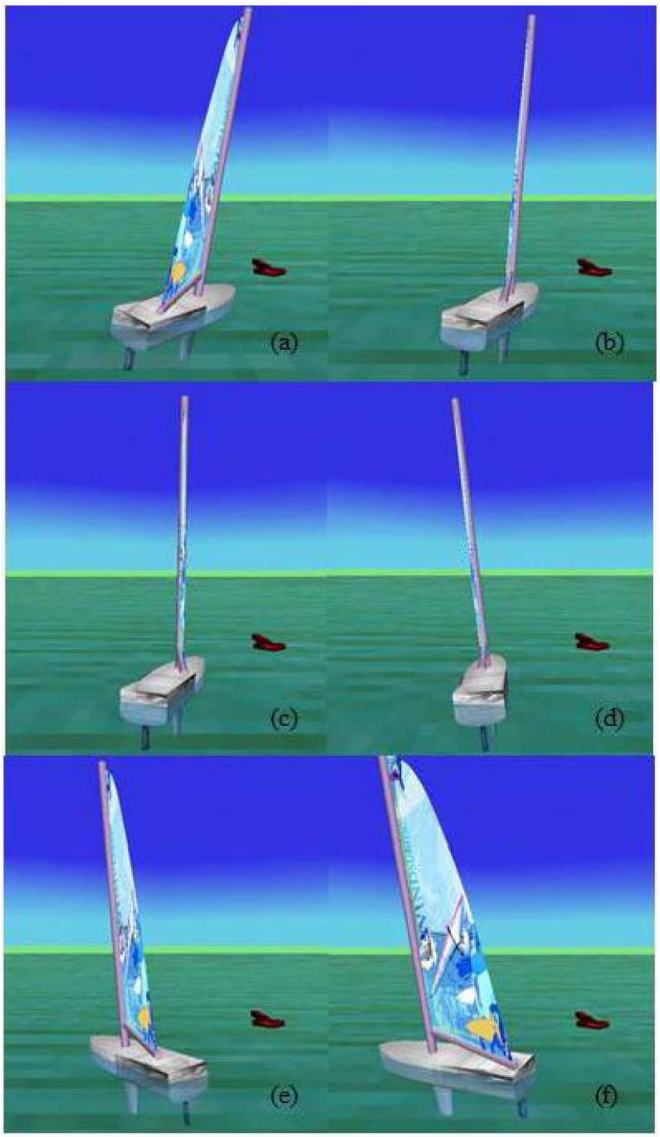

Fig. 5. Video capture of our 3-D simulation environment for the proposed yacht model performing a tack.

K_{yaw} to $-2(I_{zz} - N_{\dot{r}})$, such that the overshoot is under 5° and make the system more stable.

IV. Simulation Results

The feedback control laws derived in Section III were simulated in Matlab Simulink for a 12-m class yacht, whose behaviors are visualized in a 3-D graphic environment where the direction of the wind is indicated by a red arrow (see Figs. 4 and 5 for a video capture showing the proposed model performing a tack maneuver). All the parameters and coefficients are given in the Appendix and are taken from [38].

Performances of the heading controller derived from (44) are shown in Figs. 6 and 7, with the desired heading $\psi_d = 90°$. Both simulations were started with initial values $[x, y, \phi, \psi, u, v, p, r]^T(0) = [0, 0, 0, -\pi/2, 5, 0, 0, 0]^T$, with one simulating a tacking maneuver (Fig. 6), while the other simulating a jibe (Fig. 7). As can be seen in Fig. 6(d), the rudder first turns right (with δ_r positive) and it maintains at $\delta_r(\infty) =$

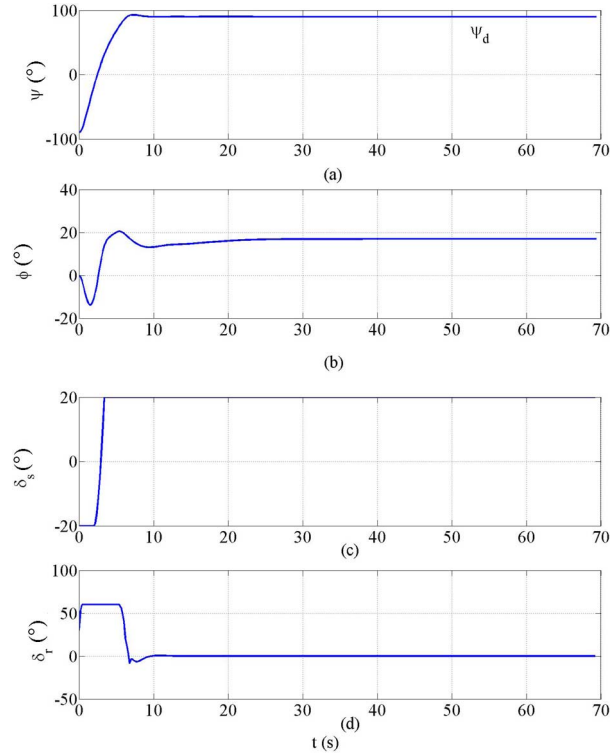

Fig. 6. Time evolutions of ψ, ϕ, δ_s, and δ_r in a tacking maneuver.

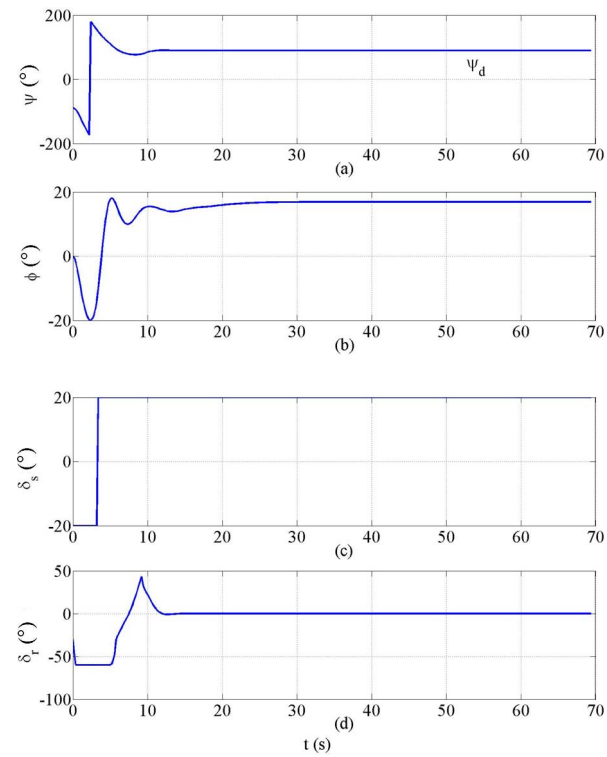

Fig. 7. Time evolutions of ψ, ϕ, δ_s, and δ_r in a jibing maneuver.

0.1375° after the yacht crosses the no-go zone and reaches ψ_d. Alternatively, in Fig. 7(d), the rudder angle goes from negative to positive, meaning that the yacht turns left at the beginning, thus resulting in a jibe. The differences are also shown in the time evolutions of $\delta_s(t)$. The sail angle changes from $-\bar{\delta}_s$ to $\bar{\delta}_s$ continuously due to the no-go zone, as indicated in Fig. 6(c), which happens during the time period 2–3.4 s. On the other

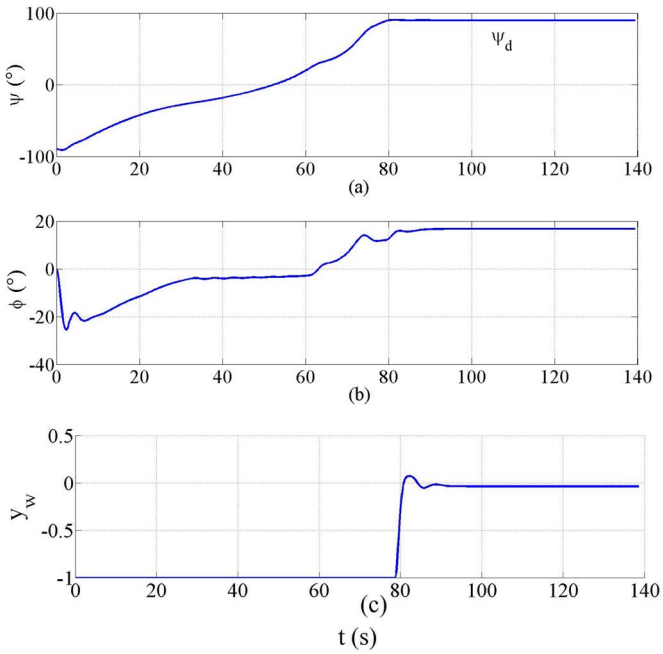

Fig. 8. Time evolutions of ψ, ϕ, and y_w with an internal moving mass.

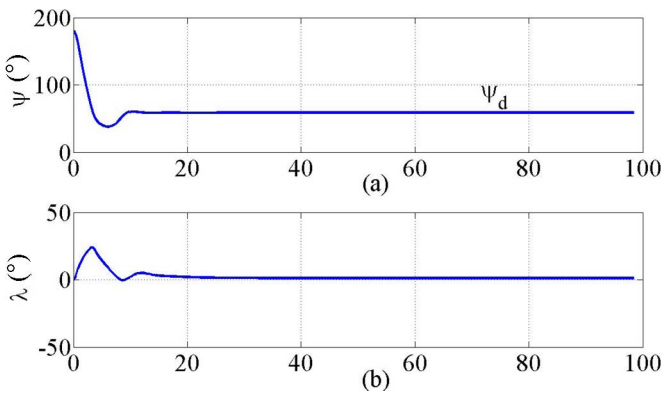

Fig. 9. Time evolutions of ψ and λ for course control.

hand, the sail changes the side in one step size (i.e., 0.2 s) in Fig. 7(c).

Figs. 6(a) and 7(a) show that $\psi(t)$ eventually converges to the desired heading with an error $\tilde{\psi} = \psi - \psi_d = -0.0080°$ due to the differences between the simulation model and the control plant model. Similar results can be obtained from the simulation that $\tilde{\psi}(\infty)$ =0.4791° under the same condition by using our parameter tuning method and the control law in (60), thus showing the good behavior of the controllers for both model simplifications and dominations on system characteristic coefficients. Figs. 6(b) and 7(b) show that the final roll angle is not zero, as expected from the normal behavior of a yacht ($\phi(\infty) =$ 16.9194° in these two simulations).

When δ_r is set to zero, we used the transverse movable mass to turn and balance the yacht. The behavior of (49) was simulated, as shown in Fig. 8, with the same initial states as above. Results show that $\psi(\infty) = \psi_d = 90°$ and $\phi(\infty) = 16.7991°$ together with $y_w(\infty) = -0.0379$, and the error $\tilde{\psi}(\infty) = 0.4472°$ when the control law from (61) is used, which means that our design method for heading controllers is also valid for the moving mass actuator.

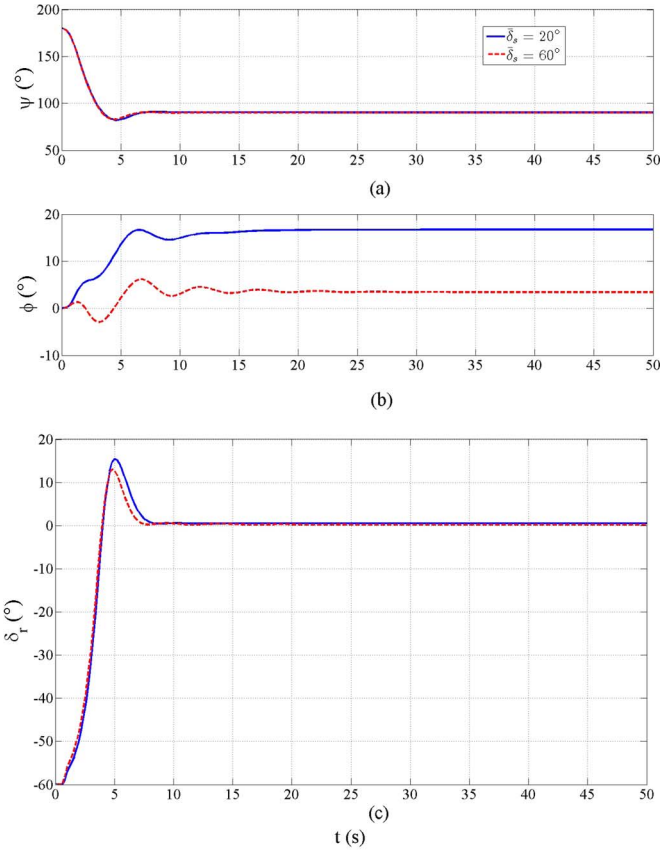

Fig. 10. Time evolutions of ψ, ϕ, and δ_r by parameter tuning in the presence of model uncertainties.

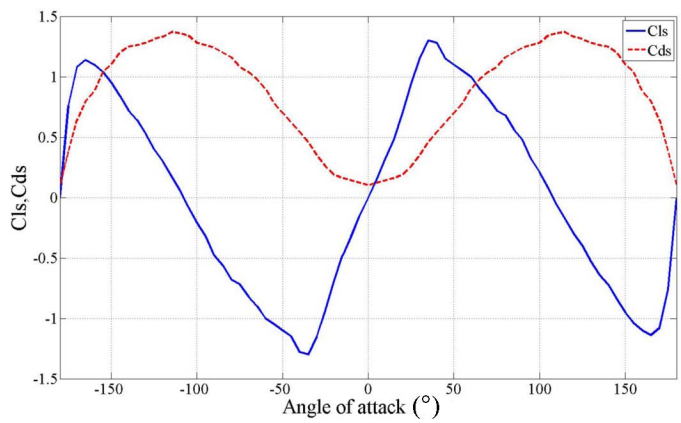

Fig. 11. Lift and drag coefficients for the sail.

For course control and following the approach sketched in Section III-D, the desired heading is first obtained numerically using `fsolve` function in Matlab, with the initial points chosen as $[u_0, v_0, \phi_0, \gamma_d, 0]^T$. Taking $\gamma_d = \pi/3$ rad, for example, we get $\psi_d = 1.0253$ rad $= 58.7454°$. Then, applying our heading controllers thus keeps the course. Fig. 9 gives $\psi(\infty) = 58.7388°$, $\lambda(\infty) = 1.2547°$, and the course $\gamma(\infty) =$ 59.9935°. The small error $\gamma(\infty) - \gamma_d = -0.0065°$ comes from the simplifications of the model used in our controller designs (recall from Section III-A).

We consider this time model uncertainties (e.g., we added 50% uncertainties on the lift/drag coefficients for the sail and rudder) to test the performance of the heading controller using the tuning method mentioned in Section III-E. The results of the

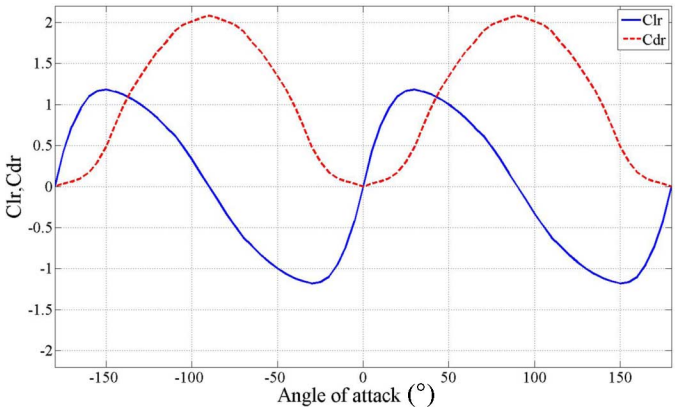

Fig. 12. Lift and drag coefficients for the rudder.

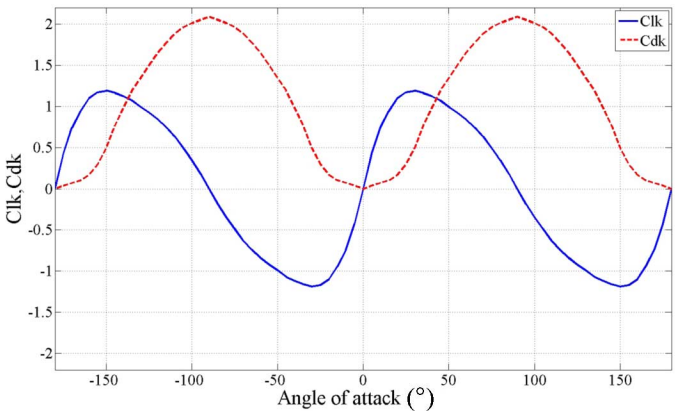

Fig. 13. Lift and drag coefficients for the keel.

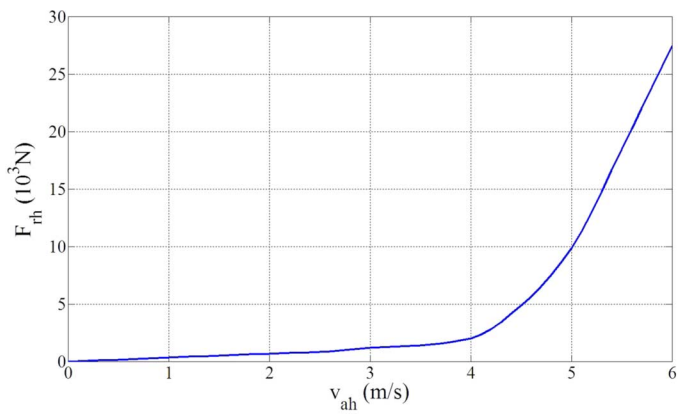

Fig. 14. Hull resistance.

model-based rudder controller with tuning parameters are illustrated in Fig. 10. Following the tuning algorithm, the parameters were tuned to $K_{\text{yaw}} = -2(I_{zz} - N_{\dot{r}}), K_{\text{ls}} = 2, K_{\text{ds}} = 1.5, K_{\text{lr}} = 3.5$ and $K_{d0} = 0.1$ such that $\tilde{\psi}(\infty) = 0.0635°$ in Fig. 10(a). Since we integrated the heeling angle into the controller designs, the roll motion has an impact on the controller. The maximum sail angle was set to $\bar{\delta}_s = 60°$ (instead of $\bar{\delta}_s = 20°$ from the Appendix for the above simulations), which resulted in much reduced heeling angle, as shown in Fig. 10(b). Accordingly, less control action is used, as can be seen in Fig. 10(c).

TABLE II
EVALUATION OF PARAMETERS

Notation	Value	Unit
m	25900	kg
I_{xx}	133690	$kg \cdot m^2$
I_{zz}	24760	$kg \cdot m^2$
I_{xz}	2180	$kg \cdot m^2$
$X_{\dot{u}}$	-970	
$Y_{\dot{v}}$	-17430	
$K_{\dot{p}}$	-106500	
$N_{\dot{r}}$	-101650	
$Y_{\dot{p}}$	13160	
$Y_{\dot{r}}$	6190	
$K_{\dot{r}}$	-4730	
v_{tw}	10(20)	$m/s(knots)$
α_{tw}	180	deg
ρ_a	1.2	kg/m^3
A_s	170	m^2
x_s	0	m
y_s	0	m
z_s	-11.58	m
x_{sm}	0.6	m
x_m	0.3	m
AR_s	3	
ρ_w	1025	kg/m^3
A_r	1.17	m^2
x_r	-8.2	m
y_r	0	m
z_r	-0.78	m
AR_r	4.94	
A_k	8.7	m^2
x_k	0	m
y_k	0	m
z_k	-0.58	m
AR_k	1	
x_h	0	m
y_h	0	m
z_h	-1.18	m
a	-5.89	
b	8160	
c	120000	
d	20000	
m_w	16000	N
y_{bmax}	1.8	m
x_w	-8	m
$\bar{\delta}_s$	20	deg

V. CONCLUDING REMARKS

In this paper, a four-DOF mathematical model describing the dynamic motion of a sailing yacht was described using Fossen's vectorial representation, including a movable mass system used as an alternative way of steering. The integrator backstepping approach is employed to perform heading control for the sailing vehicle, and the state of the heading system is exponentially stabilized by feedback using only the rudder or the mass position as a control input. Additionally, course control can also be achieved. Finally, we derive a heading controller that is less dependent on the yacht's main characteristics. Our model and controllers are readily available for further testing and are applicable to other yachts by just replacing the parameters and data with that from wind tunnel and towing tank tests.

Current directions of research include integration of automatic sail trimming into our controllers, and controllability issues related to the moving mass actuation system.

APPENDIX

We give here a detailed list of parameters for a 12-m class yacht in Table II, lift and drag coefficient curves (see Figs. 11–13), and hull resistance (see Fig. 14) taken from [38].

REFERENCES

[1] N. Cruz and J. Alves, "Autonomous sailboats: An emerging technology for ocean sampling and surveillance," in *Proc. OCEANS Conf.*, Sep. 2008, DOI: 10.1109/OCEANS.2008.5152113.

[2] R. Stelzer, T. Proll, and R. John, "Fuzzy logic control system for autonomous sailboats," in *Proc. IEEE Int. Fuzzy Syst. Conf.*, Jul. 2007, DOI: 10.1109/FUZZY.2007.4295347.

[3] E. Yeh and J. Bin, "Fuzzy control for self-steering of a sailboat," in *Proc. Singapore Int. Conf. Intell. Control Instrum.*, Feb. 1992, vol. 2, pp. 1339–1344.

[4] A. Tiano, A. Zirilli, C. Yang, and C. Xiao, "A neural autopilot for sailing yachts," presented at the 9th Mediterranean Conf. Control Autom., Croatia, Jun. 27–29, 2001.

[5] R. Van Aartrijk, C. Tagliola, and P. Adriaans, "AI on the ocean: The robosail project," in *Proc. 15th Eur. Conf. Artif. Intell.*, 1999, pp. 653–657.

[6] N. Cruz and J. Alves, "Auto-heading controller for an autonomous sailboat," in *Proc. IEEE OCEANS Conf.*, Sydney, Australia, May 2010, DOI: 10.1109/OCEANSSYD.2010.5603882.

[7] G. Elkaim and R. Kelbley, "Station keeping and segmented trajectory control of a wind-propelled autonomous catamaran," in *Proc. 45th IEEE Conf. Decision Control*, Dec. 2006, pp. 2424–2429.

[8] L. Xiao and J. Jouffroy, "Modeling and nonlinear heading control for sailing yachts," in *Proc. IEEE OCEANS Conf.*, 2011, pp. 1–6.

[9] Y. Masuyama, T. Fukasawa, and H. Sasagawa, "Tacking simulation of sailing yachts—Numerical integration of equations of motion and application of neural network technique," in *Proc. 12th Chesapeake Sailing Yacht Symp.*, 1995, pp. 117–131.

[10] M. Hamamoto and T. Akiyoshi, "Study on ship motions and capsizing in following seas," *J. Soc. Naval Architects Jpn.*, vol. 163, pp. 173–180, May 1988.

[11] K. Nomoto, Y. Masuyama, and A. Sakurai, "Sailing performance of "Naniwa-maru," a full-scale reconstruction of sailing trader of Japanese heritage," in *Proc. 15th Chesapeake Sailing Yacht Symp.*, 2001, pp. 135–146.

[12] Y. Masuyama, K. Nomoto, and A. Sakurai, "Numerical simulation of maneuvering of "Naniwa-maru," a full-scale reconstruction of sailing trader of Japanese heritage," in *Proc. 16th Chesapeake Sailing Yacht Symp.*, 2003, pp. 174–181.

[13] J. Keuning, K. Vermeulen, and E. de Ridder, "A generic mathematical model for the maneuvering and tacking of a sailing yacht," in *Proc. 17th Chesapeake Sailing Yacht Symp.*, Mar. 2005, pp. 143–163.

[14] T. Fossen, *Guidance and Control of Ocean Vehicles*. New York, NY, USA: Wiley, 1994.

[15] T. Fossen, *Marine Control Systems: Guidance, Navigation and Control of Ships, Rigs and Underwater Vehicles*. Trondheim, Norway: Marine Cybernetics, 2002.

[16] T. Fossen and A. Grovlen, "Nonlinear output feedback control of dynamically positioned ships using vectorial observer backstepping," *IEEE Trans. Control Syst. Technol.*, vol. 6, no. 1, pp. 121–128, Jan. 1998.

[17] N. Leonard and J. Graver, "Model-based feedback control of autonomous underwater gliders," *IEEE J. Ocean. Eng.*, vol. 26, no. 4, pp. 633–645, Oct. 2001.

[18] A. Bender, D. Steinberg, A. Friedman, and S. Williams, "Analysis of an autonomous underwater glider," in *Proc. Australasian Conf. Robot. Autom.*, 2008, pp. 1–10.

[19] N. Benatar, O. Qadir, J. Owen, P. Baxter, and M. Neal, "P-controller as an expert system for manoeuvring rudderless sail boats," presented at the U.K. Workshop Comput. Intell., Nottingham, U.K., Sep. 7–9, 2009.

[20] C. Westerman, "Rudderless sailboat," U.S. Patent 4 819 574, 1989.

[21] J. Bertin, *Aerodynamics for Engineers*. Englewood Cliffs, NJ, USA: Prentice-Hall, 2002.

[22] I. Abbott and A. Doenhoff, *Theory of Wing Sections: Including a Summary of Airfoil Data*, ser. Books on Physics and Chemistry. New York, NY, USA: Dover, 1959.

[23] F. Fossati, *Aero-Hydrodynamics and the Performance of Sailing Yachts*. New York, NY, USA: Int. Marine/McGraw-Hill, 2009.

[24] A. Philpott, R. Sullivan, and P. Jackson, "Yacht velocity prediction using mathematical programming," *Eur. J. Oper. Res.*, vol. 67, pp. 13–24, 1993.

[25] C. Marchaj, *Aero-Hydrodynamics of Sailing*. Frome, U.K.: Butler & Tanner, 1990.

[26] J. Keuning and K. Vermeulen, "On the yaw balance of large sailing yachts," presented at the 17th Int. HISWA Symp. Yacht Design Constr., Amsterdam, The Netherlands, Nov. 2002.

[27] T. Fossen, "A nonlinear unified state-space model for ship maneuvering and control in a seaway," *Int. J. Bifurcat. Chaos Appl. Sci. Eng.*, vol. 15, no. 9, pp. 2717–2746, Sep. 2005.

[28] C. Carletti, A. Gasparri, S. Longhi, and G. Ulivi, "Simultaneous roll damping and course keeping via sliding mode control for a marine vessel in seaway," in *Proc. 18th World Congr./Int.l Fed. Autom. Control*, Milano, Italy, 2011, pp. 13 648–13 653.

[29] H. Sussmann, *Nonlinear Controllability and Optimal Control*, ser. Pure and Applied Mathematics. New York, NY, USA: Mercel Dekker, 1990.

[30] S. Sastry, *Nonlinear Systems: Analysis, Stability, and Control*. New York, NY, USA: Springer Science+Business Media, 1999.

[31] P. Kokotovic, "The joy of feedback: Nonlinear and adaptive," *IEEE Control Syst.*, vol. 12, no. 3, pp. 7–17, Jun. 1992.

[32] H. Khalil, *Nonlinear Systems*, 3rd ed. Englewood Cliffs, NJ, USA: Prentice-Hall, 2002.

[33] A. Ross, T. Perez, and T. Fossen, "A novel manoeuvering model based on low-aspect-ratio lift theory and Lagrangian mechanics," in *Proc. 7th IFAC Conf. Control Appl. Mar. Syst.*, 2007, pp. 229–234, DOI: 10.3182/20070919-3-HR-3904.00041.

[34] K. Astrom and R. Murray, *Feedback Systems*. Princeton, NJ, USA: Princeton Univ. Press, 2008.

[35] K. Ang, G. Chong, and Y. Li, "PID control system analysis, design, and technology," *IEEE Trans. Control Syst. Technol.*, vol. 13, no. 4, pp. 559–576, Jul. 2005.

[36] M. Brown, R. Camarena, and D. Marschalk, "Land yacht aerodynamic performance San Diego State Univ., La Jolla, CA, USA, Tech. Rep., 1994.

[37] Y. Briere, "Iboat: An autonomous robot for long-term offshore operation," in *Proc. 14th IEEE Mediterranean Electrotech. Conf.*, May 2008, pp. 323–329.

[38] N. Davies, "A real-time yacht simulator," M.S. thesis, Dept. Eng. Sci., Univ. Auckland, Auckland, New Zealand, 1990.

Lin Xiao was born in Changde, China, in 1985. She received the M.Sc. degree in engineering, mechatronics and the Ph.D. degree in engineering, applied mathematical modeling from the University of Southern Denmark (SDU), Sønderborg, Denmark, in 2009 and 2012, respectively.

In 2009–2012, she was working on the modeling and nonlinear autonomous control for a class of sailing vehicles. Her research interests include mathematical modeling, nonlinear control, and its applications in sailing systems.

Jerome Jouffroy received the Diplome d'Etudes Approfondies in applied control systems and the Ph.D. degree in control systems from the University of Savoie, Annecy, France, in 1999 and 2002, respectively.

From 2002 to 2003, he worked as a Research Engineer at the French Institute for Ocean Research (IFREMER), Toulon, France, on navigation algorithms for underwater vehicles. Between 2003 and 2006, he was a Postdoctoral Fellow at the Center for Ships and Ocean Structures (CeSOS), Norwegian University of Science and Technology (NTNU), Trondheim, Norway. Since 2007, he has been an Associate Professor in Control at the Mads Clausen Institute, University of Southern Denmark (SDU), Sønderborg, Denmark. His research interests include nonlinear control and estimation, cooperative control, with applications to autonomous vehicles, sailing systems, and power electronics.